iJRASET
International Journal For Research in Applied Science and Engineering Technology

INTERNATIONAL JOURNAL FOR RESEARCH

IN APPLIED SCIENCE & ENGINEERING TECHNOLOGY

Volume: 6 **Issue:** VI **Month of publication:** June 2018

DOI: http://doi.org/10.22214/ijraset.2018.6140

www.ijraset.com

Call: 08813907089 | E-mail ID: ijraset@gmail.com

International Journal for Research in Applied Science & Engineering Technology (IJRASET)
ISSN: 2321-9653; IC Value: 45.98; SJ Impact Factor: 6.887
Volume 6 Issue VI, June 2018- Available at www.ijraset.com

Solar Light Induced Degradation of Methylene Blue using Novel $Co_3V_2O_8$ /TiO_2 Nanocomposite

S. Rajendra Prasad[1], S. Srikantaswamy[2], K. Jagadish[3], M. R. Abhilash[4], M. B. Nayan[5], K. Byrappa[6]
[1]*Department of Studies in Chemistry, University of Mysore, Manasagangotri, Mysore 570006, India*
[2] *Department of Studies in Environmental Science, University of Mysore, Manasagangotri, Mysore 570006, India*
[3] *Centre for Materials Science and Technology, Vijnana Bhavan, University of Mysore, Manasagangotri, Mysore 570006, India*

Abstract: ***Novel $Co_3V_2O_8$ /TiO_2 nanocomposite was synthesized by simple and cost effective route Hydrothermal method. As synthesized nanocomposites were characterized by different advanced analytical techniques such as X-ray diffraction (XRD), Scanning electron microscope (SEM), energy dispersive X-ray spectrometer (EDX), Dynamic light scattering (DLS), Fourier Transform Infrared spectrophotometer (FTIR) and UV-Visible spectrophotometer for the investigation of crystalline, morphology, elemental percentage, particle size distribution, functional group and optical properties respectively. Further the photo-catalytic properties of as synthesized $Co_3V_2O_8$ /TiO_2 nanocomposite were characterized by using Tauc plot (3.02 band gap energy). It was found that the methylene blue dye degraded to 85 percentage in the presence of photocatalyst $Co_3V_2O_8$ /TiO_2 nanocomposite under solar light irradiation.***
Key words: Hydrothermal, nanocomposite, photocatalytic, methylene blue

I. INTRODUCTION

Nowadays environmental pollution and health has become the two big serious issues for the future of world. It is necessary to avoid water pollution, which is the most important crisis for the environmental hazardous using different technology. Photo-catalysis is the very significant process by using photocatalyst, which can easily reduce the level of pollutants in aqueous system. The photocatalyst with reduced size, in nanometer scale it can effectively utilized for the photocatalyst and the litereature proved that the nano-photocatalyst shows maximum photocatalytic performance.

The higher surface are of the nano material is helpful for the adsorption of pollutant and oxidized to highly stable inorganic substances, which are harmless to the living things. According to Henglein, the nanomaterial can shows effective behavior when compare to bulk material [1].

Surface to volume ratio of nano particles is more, and it leads to high surface energy.

The TiO_2 was most widely used photocatalyst, in different industries which was easily available [2, 3]. The band gap energy of TiO_2 was 3.2 eV, which has larger energy and it needs high light energy for the excitation electron between valence bond and conduction band. Therefore, this wide band gap energy of TiO_2 caused researcher to think more or other photocatalysts materials for the lower band gap energy. And also they tried to synthesis visible light active photocatalyst, which can able to destruct organic molecules. The researcher found large number photocatalyst for the lower band gap energy such as $BiVO_4$ [4, 5], $FeVO_4$ [6, 7], $AgVO_3$ [8, 9], Ag_3VO_4 [10, 11], $Cu_3V_3O_8$ [12, 13] and $Zn_3V_2O_8$ [14, 15].

The metal oxides shows excellent photocatalytic properties and also the vanadates are also shows the different band gap energy which was helpful for the degradation of pollutants. Among vanadates family, cobalt vanadate gain interest for the destruction of pollutants.

There are several cobalt vanadates used for the photocatalytic applications like $Co_3V_2O_8$ [16, 17], $Co_2V_2O_7$ [18, 19] and CoV_2O_6 [20, 21]. There are different types of synthesis methods of cobalt vanadates such as precipitation [22], solid-state [23], sol-gel [24], hydrothermal [25, 26] and electrospinning [27]. These types of vanadates has many advantages in different fields such as electrode, supercapacitor, batteries and water oxidation processes [28-31].

Here, for the first time the composite of $Co_3V_2O_8$/TiO_2 particle were synthesized by simple hydrothermal method. The synthesized particle was examined with different advanced instruments for the investigation of basic properties like crystalinity, morphology, particle size elemental analysis.

It has been demonstrated that the synthesized composite was used for the destruction of organic pollutants present in the water. The ability of synthesized photocatalyst for the destruction of methylene blue dye, under solar light irradiation was investigated. The results show high photocatalytic efficiency for the destruction of dyes present in the water system.

ISSN: 2321-9653; IC Value: 45.98; SJ Impact Factor: 6.887
Volume 6 Issue VI, June 2018- Available at www.ijraset.com

II. EXPERIMENTAL

A. *Materials*

All the chemicals and reagents such as Cobalt chloride hexa hydrate, Sodium metavanadate and Titanium dioxide were of analytical grade purchased from SRL laboratory India Pvt. Ltd. and used without further purification.

B. *Synthesis of $Co_3V_2O_8/TiO_2$ Nanocomposite*

The synthesis of nanocomposite was carried out by simple, cost effective hydrothermal method. In a typical procedure, 3 mmol of $CoCl_2.6H_2O$ was dissolved in 20ml distilled water and 20 ml of 2 mmol of $Na_3VO_4.12\ H_2O$ was added drop wise to the above cobalt solution. The suspension was stirred for 30 minutes at constatnt temperature 75 ^oC. Later the 20 ml 3 mmol of TiO_2 was added to the suspension and stirring was continued for further 20 minutes. Finally the obtained 18 ml suspension was transferred to Teflon liner (20 ml capacity) and fixed with stainless steel autoclave. The autoclave was placed in hot air oven at the constant temperature of 160 ^oC for the duratipon of 4 hours. Later the autoclave was cooled down to room temperature and the brown colour solid was washed with water, filtered and dried at 60 ^oC.

C. *Characterization Technique*

Crystallite structures were determined by X-ray diffraction (XRD) using a Rigaku desktop diffractometer (Japan) with Cu Ka radiation (l ¼ 0.15418 nm) operating at 40 kV and
150 mA. The microstructure and morphology of the materials were characterized using a scanning electron microscope (SEM-2010, Japan) operating at an accelerating voltage of 200.0 kV. The EDX analysis was carried out with 20 kV accelerated voltage was done. Brunauer–Emmett–Teller (BET) formulations were used to calculate the surface area. The diffraction angle (2θ) range between 6° and 80° was scanned. The Fourier transform infrared spectroscopy (FT-IR) spectrums were obtained within the range 200–4,000 cm−1 region on a spectrophotometer (Spectrum 100, Perkin Elmer) using KBr as binders. The samples were characterized by UV–visible spectrophotometer (Shimizu UV–1,650 PC) for wavelength-dependent absorption spectrum. The particle size distributin of composite was carried out by DLS (Microtrac-nanotrac wave-w 3231 Instruments Ltd., at a fixed scattering angle of 90 at room temperature) analytical instruments.

III. RESULTS AND DISCUSSION

A. *X-ray Diffraction*

The crystalline phases of $Co_3V_2O_8/TiO_2$ nanocomposite were carried out by XRD as shown by Figure (1). The diffraction angles of 2θ values 34.5, 42.5, and 61^o were having plane of 122, 042 and 442 respectively. These results were in good agreement with the standard XRD pattern of $Co_3V_2O_8$ (JCPDS no. 74-1487). The diffraction angle of 2θ values, 25.5, 37.5 and 48^o was attributed to the different planes of 101, 004 and 200 respectively. These crystalline datas were has good agreement with the standard XRD pattern of TiO_2. It was demonstrated that the synthesized composite have crystalline properties of both $Co_3V_2O_8$ and TiO_2, and confirmed that the formation of composite under hydrothermal reaction.

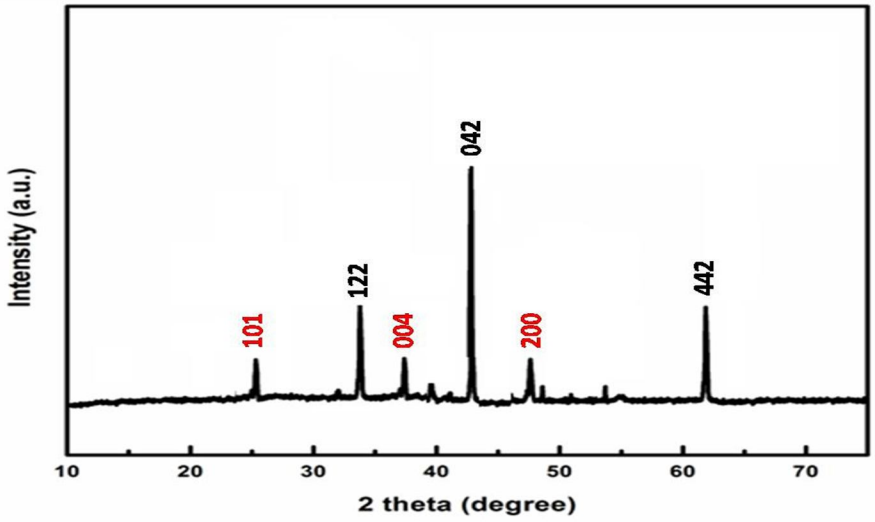

Figure 1: XRD spectrum $Co_3V_2O_8/TiO_2$ nanocomposite

B. FTIR Analysis

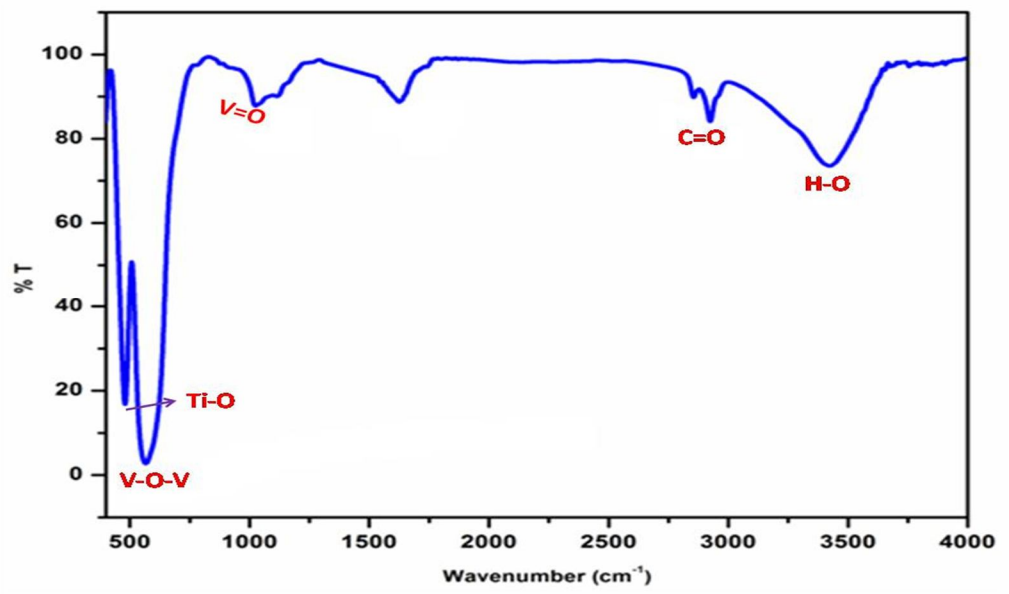

Figure 2: FTIR spectrum of $Co_3V_2O_8/TiO_2$ nanocomposite

In order to get physical insights of the chemical bonding and phase formation, we also studied the structure by FTIR spectroscopy. FTIR spectroscopic technique is powerful for investigating the local structure and environment in oxides [32, 33]. The FTIR spectrum of crystalline $Co_3V_2O_8/TiO_2$ was shown in the figure 2 that it contains main absorption bands at the far infrared region at 279 cm^{-1}, which confirms the unique fingerprint of the Co site in the octahedron crystal structure of $Co_3V_2O_8$. The absorption band at 854 cm^{-1} may be assigned to V=O stretching mode of $Co_3V_2O_8$. The absorption bands in the region of 500 to 700 cm^{-1} were due to the symmetric and asymmetric stretching band of V-O-V bonds. The bands at 386 cm^{-1} can be assigned to the stretching mode of Co–O modes. The sharp absorption peaks around 1,110 cm^{-1}, which is due to the vibrations of the cobalt vanadate crystal lattice. The results of FTIR analysis were good agreement with XRD results also. However the absorption band at 551 cm^{-1} confirms the presence of TiO_2 and finally these results were attributed to the properties of $Co_3V_2O_8/TiO_2$ nanocomposite [34].

C. SEM Analysis

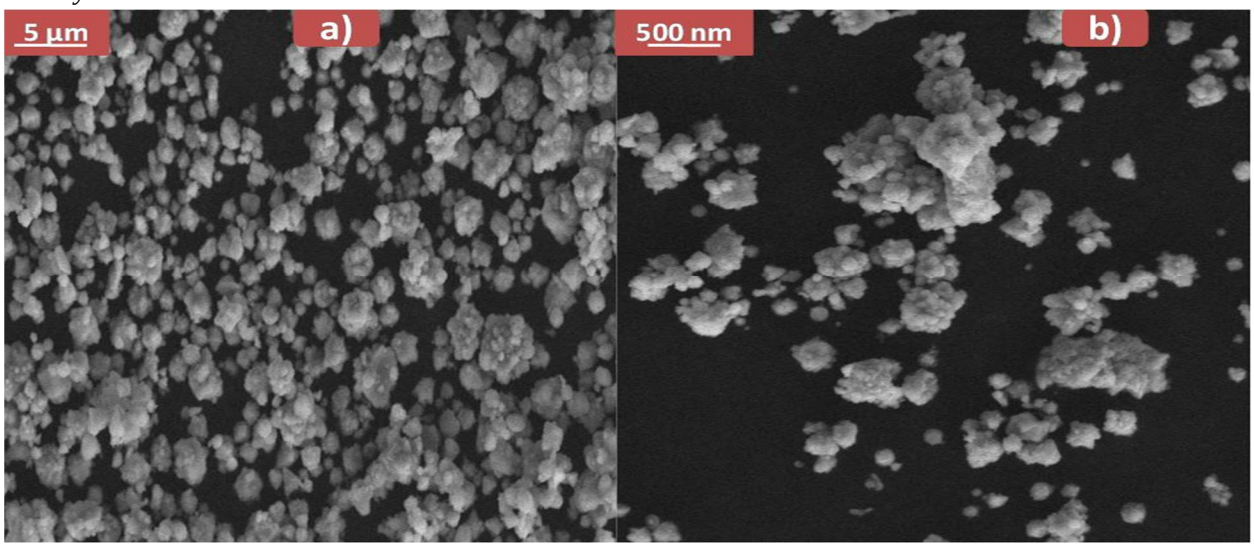

Figure 3: SEM image of $Co_3V_2O_8/TiO_2$ nanocomposite

The surface morphology of the as synthesized $Co_3V_2O_8/TiO_2$ nanocomposite materials were examined by SEM. Figure 3 shows the typical SEM images of composite with different magnifications. The SEM images of composite shows the particle size 50-100 nm

and reveal that the particle are uniform with very smooth surface. The particle of composites was separated from each other, and these separated particles can show high surface area with good photocatalytic properties. In these nanocomposites, there are many mesoporous structures with average pore diameter of 20 nm. The BET surface area of nanocomposite was found to be 95.5 m^2g^{-1}, which was considerably effective for the adsorption processes and photocatalytic applications. The higher surface area enhances the exposure of active sites available for the photochemical reaction on the surface of composites.

D. Particle Size Distribution Of $Co_3v_2o_8/Tio_2$ Nanocomposite

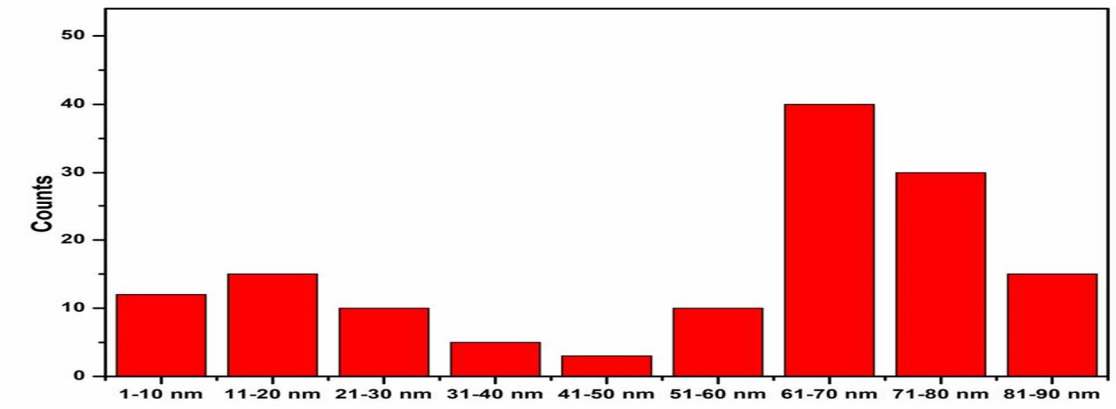

Figure 4: Particle size distribution of $Co_3V_2O_8/TiO_2$ nanocomposite

The particle size of $Co_3V_2O_8/TiO_2$ nanocomposite was analyzed by using DLS instrument (Figure 4). DLS is the very useful method for investigating size of nanomaterials in which the composite was dispersed in suitable solvent (Water). This analysis was based upon the Brownian motion of particles in the solvent, in which the composite was ultrasonicated before analysis. The nanocomposite found to be average particle size 68 nm distributed in solvent. These results were suggested that the particle were dispersed well in the solvent molecules without such agglomeration. This indicate that the stability of composite, which were dispersed and stable up to sometime duration.

E. Elemental Analysis

The synthesized nanocomposite was analyzed for the instigation of percentage of elements present in the composite molecules. This analysis was carried out by using EDX spectrometer, which was based on the energy dispersive X-ray spectrometer (Figure 5). Basically it contains the elements such as Co, O, V and Ti, but in this analysis it was necessary to investigate the presence or absence of impurities in the composite. The results show that the composite doesn't contains any impurities because all the impurities were removed by post treatment of product by washing and drying. And also it shows that highest mass and weight percentage found to be Cobalt element (64) and lowest element was Vanadium (21).

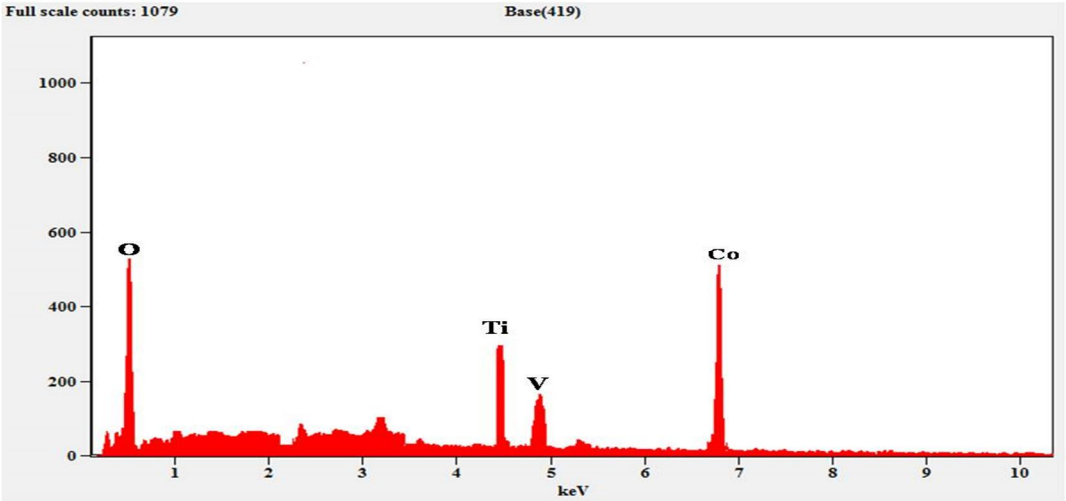

Figure 5: EDX spectrum of $Co_3V_2O_8/TiO_2$ nanocomposite

ISSN: 2321-9653; IC Value: 45.98; SJ Impact Factor: 6.887
Volume 6 Issue VI, June 2018- Available at www.ijraset.com

F. Optical Properties

The optical properties of a material are very important in some applications such as optical coatings, reflectors, absorbers, and various optoelectronic devices. UV-Vis absorption spectroscopy was carried out for the investigation of optical properties and energy structures including band gap of $Co_3V_2O_8/TiO_2$ nanocomposite. In this study, UV–visible absorption spectrum of the $Co_3V_2O_8/TiO_2$ nanocomposite was recorded using a UV–visible spectrophotometer in the photon wavelength range 200–800 nm. Figure 6 shows the UV-Vis absorption spectrum of nanocomposite. The absorption peak was found in the ultraviolet region at ~310 nm, which reveal that the absorption of $Co_3V_2O_8/TiO_2$ nanocomposite.

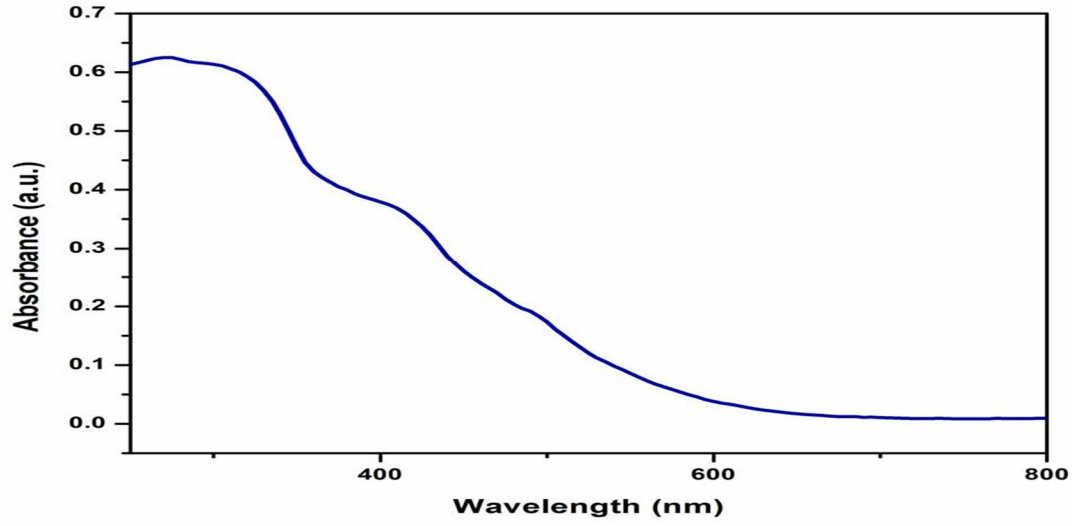

Figure 6: UV Vis spectrum of $Co_3V_2O_8/TiO_2$ nanocomposite

Band gap energy of $Co_3V_2O_8/TiO_2$ nanocomposite:

The band gap energy of a semiconductor may be calculated from eqn (1).

$\alpha h\nu = A(h\nu - Eg)n/2$ ……. (1)

Where α, h, ν, Eg and A are the absorption coefficient, the Planck's constant, the light frequency, band gap energy, and a proportionality constant, respectively. The exponent n is determined by the type of optical transition of a semiconductor (n= 1 for direct transition and n = 4 for indirect transition). Thus, the band-gap energies (Eg) of the samples could be estimated from plots of $(\alpha h\nu)^{2/n}$ versus the photon energy (hν). According to Figure 7 the nanocomposite $Co_3V_2O_8/TiO_2$ possessed band gap energy of approximately 3.02 eV which is lower than the band gap energy of both pure $Co_3V_2O_8$ (2.85 eV) and pure TiO_2 (3.15 eV). This observation is important, as it indicates that the $Co_3V_2O_8/TiO_2$ nanocomposites can be photoexcited to generate more electron−hole pairs under visible-light irradiation, which could result in higher photocatalytic performance.

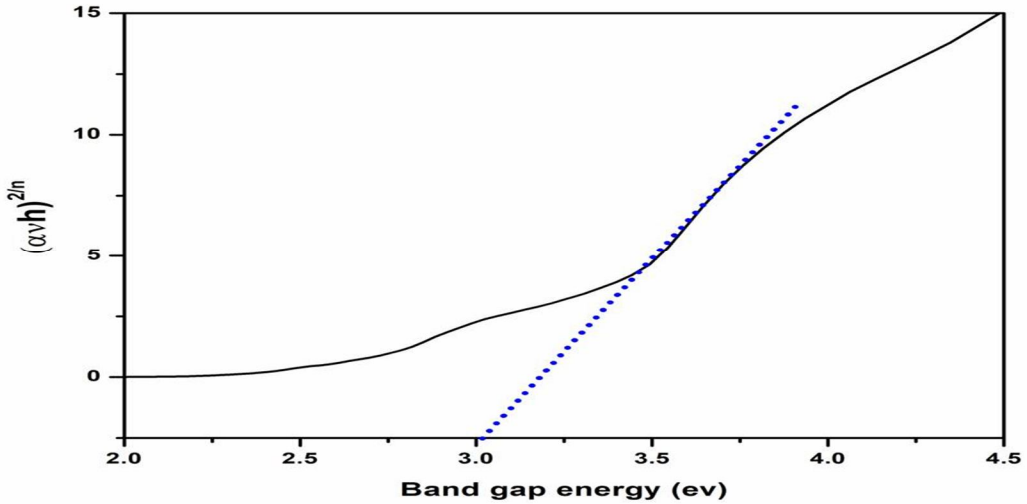

Figure 7: Band gap energy of $Co_3V_2O_8/TiO_2$ nanocomposite

G. Photocatalytic Activity of $Co_3V_2O_8/TiO_2$ Nanocomposite

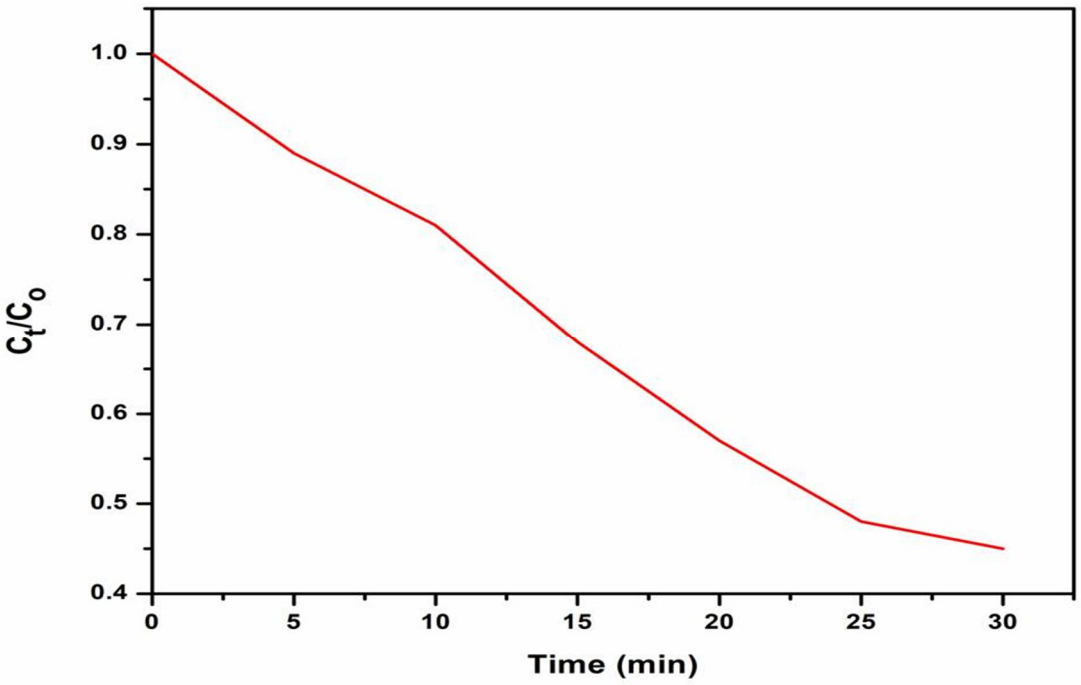

Figure 8: photodegradation efficiency of MB using $Co_3V_2O_8/TiO_2$ nanocomposite:

The photocatalytic activities of $Co_3V_2O_8/TiO_2$ nanocomposite photocatalysts were evaluated by measuring the decoloration of MB under visible light irradiation (>400 nm). The concentrations (C) of MB were determined from UV−vis absorption studies by using the Beer−Lambert law relation at the maximum wavelength (λ_{max}) of 664.5 nm. Variations of MB concentration (C_t/C_0) with solar-light irradiation time over different catalysts are presented in Figure 8.

IV. CONCLUSION

The $Co_3V_2O_8/TiO_2$ nanocomposite was reported as a photocatalyst for the first time. Because of high surface area, low particle size with more pore structure, it was considered as the best photocatalyst for the degradation of methylene blue dye present in the wastewater. The high crystalline properties, smooth surfaces of synthesized nanocomposite succeeded in the activity as a semiconductor with optimum band gap. The band gap energy was calculated by plotting Tauc plot and investigated the properties in photocatalysis. Further the efficiency of as synthesized composite as a photocatalys shows the high activity towards the degradation of organic waste present in water.

REFERENCES

[1] Henglein, Mechanism of reactions on colloidal microelectrodes and size quantization effects Top. Curr. Chem. 143 (**1988**) 113–180.
[2] O. Elbanna, P. Zhang, M. Fujitsuka, T. Majima, Facile preparation of nitrogen and fluorine codoped TiO_2 mesocrystal with visible light photocatalytic activity, Appl. Catal. B: Environ. (**2016**), doi:10.1016/j.apcatb.2016.03.053.
[3] Y. Cao, X. Li, Z. Bian, A. Fuhr, D. Zhang, J. Zhu, Highly photocatalytic activity of brookite/rutile TiO_2 nanocrystals with semi-embedded structure, Appl. Catal. B: Environ 180 (**2016**) 551-558.
[4] X. Gao, Z. Wang, X. Zhai, F. Fu, W. Li, The synthesize of lanthanide doped $BiVO_4$ and its enhanced photocatalytic activity, J. Mol. Liq. 211 (**2015**) 25-30.
[5] Y. Geng, P. Zhang, N. Li, Z. Sun, Synthesis of Co doped $BiVO_4$ with enhanced visible-light photocatalytic activities, J. Alloys Compd. 651 (**2015**) 744-748.
[6] B. Ozturk, G.S.P. Soylu, Synthesis of surfactant-assisted $FeVO_4$ nanostructure: Characterization and photocatalytic degradation of phenol, J. Mol. Catal. A: Chem. 398 (**2015**) 65-71.
[7] J. Deng, J. Jiang, Y. Zhang, X. Lin, C. Du, Y. Xiong, $FeVO_4$ as a highly active heterogeneous Fenton-like catalyst towards the degradation of Orange II, Appl. Catal. B: Environ. 84 (**2008**) 468-473. 14
[8] V. Sivakumar, R. Suresh, K. Giribabu, V. Narayanan, $AgVO_3$ nanorods: Synthesis, characterization and visible light photocatalytic activity, Solid-State Sci. 39 (2015) 34-39.
[9] T.A. Vu, C.D. Dao, T.T. Hoang, P.T. Dang, H.T. Tran, K.T. Nguyen, G.H. Le, T.V. Nguyen, G.D. Lee, Synthesis of novel silver vanadates with high photocatalytic and antibacterial activities, Mater. Lett. 123 (**2014**) 176-180.
[10] X. Hu, C. Hu, Preparation and visible-light photocatalytic activity of Ag_3VO_4 powders, J. Solid State Chem. 180 (2007) 725-732.

[11] H. Xu, H. Li, L. Xu, C. Wu, G. Sun, Y. Xu, J. Chu, Enhanced photocatalytic activity of Ag_3VO_4 loaded with rare-earth elements under visible-light irradiation, Ind. Eng. Chem. Res. 48 (2009) 10771-10778.
[12] M. Ghiyasiyan-Arani, M. Masjedi-Arani, M. Salavati-Niasari, Novel Schiff base ligand-assisted in-situ synthesis of $Cu_3V_2O_8$ nanoparticles via a simple precipitation approach, J. Mol. Liq. 216 (2016) 59-66.
[13] M. Ghiyasiyan-Arani, M. Masjedi-Arani, M. Salavati-Niasari, Facile synthesis, characterization and optical properties of copper vanadate nanostructures for enhanced photocatalytic activity, J. Mater. Sci: Mater. Electron. (2016) 1-8.
[14] F. Mazloom, M. Masjedi-Arani, M. Ghiyasiyan-Arani, M. Salavati-Niasari, Novel sodium dodecyl sulfateassisted synthesis of $Zn_3V_2O_8$ nanostructures via a simple route J. Mol. Liq.214 (2016) 46-53.
[15] F. Mazloom, M. Masjedi-Arani, M. Salavati-Niasari, Novel size-controlled fabrication of pure $Zn_3V_2O_8$ nanostructures via a simple precipitation approach, J. Mater. Sci: Mater. Electron. 27 (2016) 1-9.
[16] M. Xiao, D. Yang, Y. Yan, Y. Tian, M. Zhou, M. Hao, R. Cheng, Y. Miao, Nanoplates and Nanospheres of $Co_3(VO_4)_2$ as Noble Metal-free Electrocatalysts for Oxygen Evolution, Electrochim. Acta. 180 (2015) 260-267.
[17] M. Xing, L.-B. Kong, M.-C. Liu, L.-Y. Liu, L. Kang, Y.-C., Cobalt vanadate as highly active, stable, noble metal-free oxygen evolution electrocatalyst, J. Mater. Chem A. 2 (2014) 18435-18443.
[18] Y. Luo, X. Xu, Y. Zhang, C.-Y. Chen, L. Zhou, M. Yan, Q. Wei, X. Tian, L. Mai, Graphene oxide templated growth and superior lithium storage performance of novel hierarchical $Co_2V_2O_7$ nanosheets, ACS Appl. Mater. Interfaces. 8 (2016) 2812-2818.
[19] H.A. Almukhlifi, R.C. Burns, Oxidative dehydrogenation of isobutane to isobutene by pyrovanadates, $M_2V_2O_7$, where M (II)= Mn, Co, Ni, Cu and Zn, and Co_2VO_4 and ZnV_2O_4: The effect of gold nanoparticles, J. Mol. Catal. A: Chem. 408 (2015) 26-40.
[20] C. Mondal, A.K. Sasmal, S. Yusuf, M. Mukadam, J. Pal, M. Ganguly, T. Pal, Modified hydrothermal reaction (MHT) for CoV_2O_6 $4H_2O$ nanowire formation and the transformation to CoV_2O_6 $2H_2O$ single-crystals for antiferromagnetic ordering and spin-flop, RSC Adv. 4 (2014) 56977-56983.
[21] Y. Tang, J. Zhou, J. Liu, L. Liu, S. Liang, Facile Synthesis of Cobalt Vanadium Oxides and Their Applications in Lithium Batteries, Int. J. Electrochem. Sci. 8 (2013) 1138-1145
[22] M.-C. Liu, L.-B. Kong, L. Kang, X. Li, F.C. Walsh, M. Xing, C. Lu, X.-J. Ma, Y.-C. Luo, Synthesis and characterization of M3V2O8 (M= Ni or Co) based nanostructures: a new family of high performance pseudocapacitive materials, J. Mater. Chem A. 2 (2014) 4919-4926
[23] Z. He, T. Taniyama, M. Itoh, Y. Ueda, Flux growth and magnetic anomalies of $Co_3V_2O_8$ crystals, Cryst. Growth Des. 7 (2007) 1055-1057.
[24] F. Liu, Y. Guan, M. Dai, H. Zhang, Y. Guan, R. Sun, X. Liang, P. Sun, F. Liu, G. Lu, High performance mixed-potential type NO 2 sensors based on three-dimensional TPB and $Co_3V_2O_8$ sensing electrode, Sens. Actuators B: Chem. 216 (2015) 121-127.
[25] G. Yang, H. Cui, G. Yang, C. Wang, Self-assembly of $Co_3V_2O_8$ multilayered nanosheets: controllable synthesis, excellent li-storage properties, and investigation of electrochemical mechanism, ACS nano. 8 (2014) 4474-4487.
[26] Y. Zhang, Y. Liu, J. Chen, Q. Guo, T. Wang, H. Pang, Cobalt vanadium oxide thin nanoplates: primary electrochemical capacitor application, Sci. Rep. 4 (2014).
[27] S. Hyun, V. Ahilan, H. Kim, S. Shanmugam, The influence of $Co_3V_2O_8$ morphology on the oxygen evolution reaction activity and stability, Electrochem. Commun. 63 (2016) 44-47
[28] Y.-M. Hu, M.-C. Liu, Y.-X. Hu, Q.-Q. Yang, L.-B. Kong, W. Han, J.-J. Li, L. Kang, Design and synthesis of $Ni_2P/Co_3V_2O_8$ nanocomposite with enhanced electrochemical capacitive properties, Electrochim. Acta. 190 (2016) 1041-1049
[29] W.-B. Zhang, L.-B. Kong, X.-J. Ma, Y.-C. Luo, L. Kang, synthesis and evaluation of three-dimensional $Co_3O_4/Co_3(VO_4)_2$ hybrid nanorods on nickel foam as self-supported electrodes for asymmetric supercapacitors, J. Power Sources. 269 (2014) 61-68.
[30] S. Ni, T. Li, X. Yang, Synthesis of $Co_3(OH)_2V_2O_{7\cdot1}.7H_2O$ nanosheets and its application in lithium ion batteries, Mater. Lett. 65 (2011) 2662-2664.
[31] Y. Zhao, Y. Liu, X. Du, R. Han, Y. Ding, Hexagonal assembly of $Co_3V_2O_8$ nanoparticles acting as an efficient catalyst for visible light-driven water oxidation, J. Mater. Chem A. 2 (2014) 19308-19314
[32] Amdouni, N. (2003). Structural and electrochemical properties of $LiCoO_2$ and LiAlyCo1−yO2 (y=0.1 and 0.2) oxides: A comparative study of electrodes prepared by the citrate precursor route. Ionics, 9, 47–55. http://dx.doi.org/10.1007/BF02376536
[33] Julien, C. (2000). Local cationic environment in lithium nickelcobalt oxides used as cathode materials for lithium batteries. Solid State Ionics, 136–137, 887–896.
[34] Kim, B., Kim, B. H., Kim, K., Choi, H. C., Park, S. Y., Jeong, Y. H., & Min, B. I. (2012). Unusual magnetic properties induced by local structure in a quasi-one-dimensional Ising chain system: α-CoV2O6. Physical Review B, 85, 220, 407–220 413 (R). http://dx.doi.org/10.1103/PhysRevB.85.220407

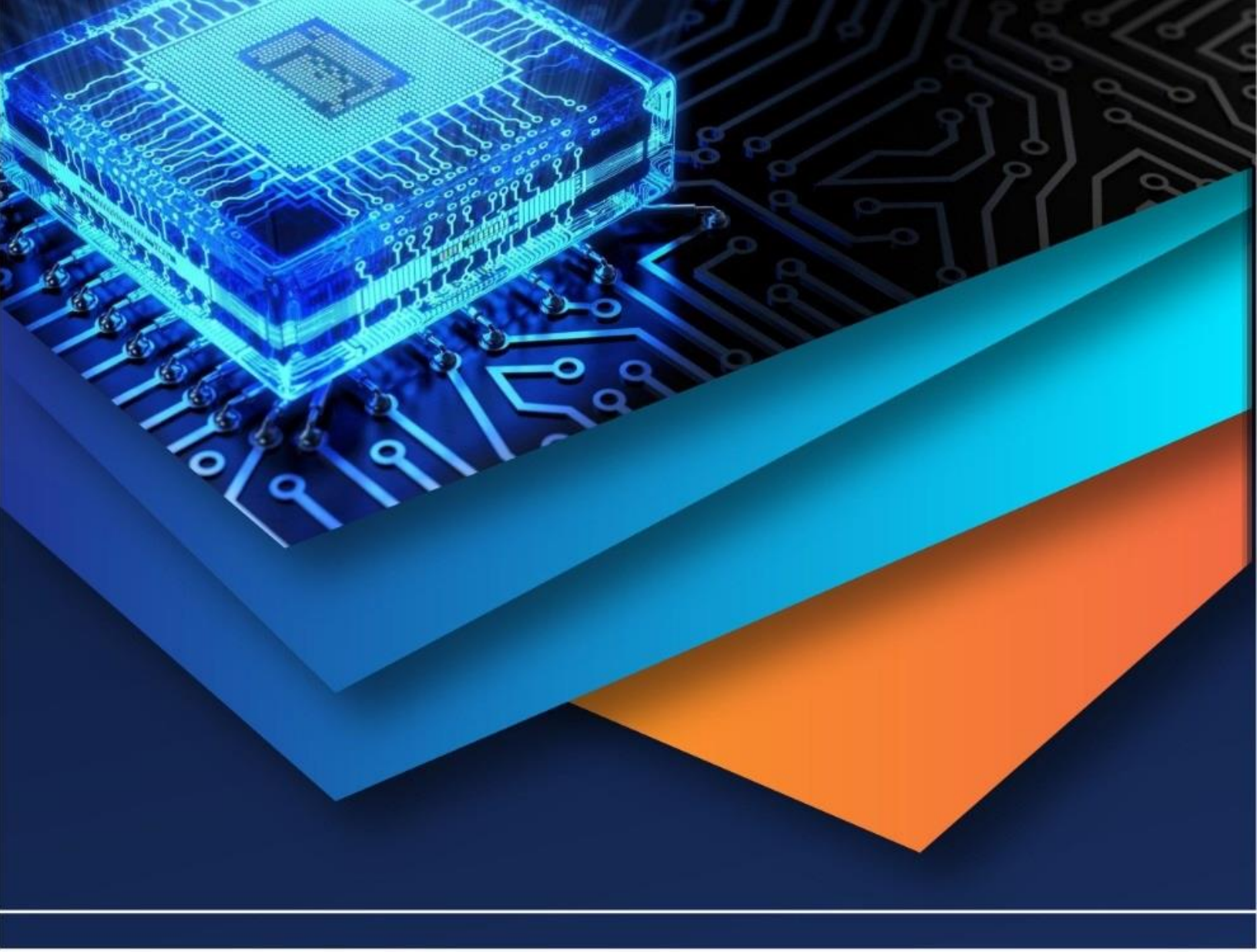

10.22214/IJRASET

45.98

IMPACT FACTOR: 7.129

IMPACT FACTOR: 7.429

INTERNATIONAL JOURNAL FOR RESEARCH

IN APPLIED SCIENCE & ENGINEERING TECHNOLOGY